A Proteasome Cap Subunit Required for Spindle Pole Body Duplication in Yeast

Heather B. McDonald and Breck Byers

Department of Genetics, University of Washington, Seattle 98195

Abstract. Proteasome-mediated protein degradation is a key regulatory mechanism in a diversity of complex processes, including the control of cell cycle progression. The selection of substrates for degradation clearly depends on the specificity of ubiquitination mechanisms, but further regulation may occur within the proteasomal 19S cap complexes, which attach to the ends of the 20S proteolytic core and are thought to control entry of substrates into the core. We have characterized a gene from *Saccharomyces cerevisiae* that displays extensive sequence similarity to members of a family of ATPases that are components of the 19S complex, including human subunit p42 and *S. cerevisiae SUG1*/*CIM3* and *CIM5* products. This gene, termed *PCS1* (for proteasomal cap subunit), is identical to the recently described *SUG2* gene (Russell, S.J., U.G. Sathyanarayana, and S.A. Johnston. 1996. *J. Biol. Chem.* 271:32810–32817). We have shown that *PCS1* function is essential for viability. A temperature-sensitive *pcs1* strain arrests principally in the second cycle after transfer to the restrictive temperature, blocking as large-budded cells with a G2 content of unsegregated DNA. EM reveals that each arrested *pcs1* cell has failed to duplicate its spindle pole body (SPB), which becomes enlarged as in other monopolar mutants. Additionally, we have shown localization of a functional Pcs1–green fluorescent protein fusion to the nucleus throughout the cell cycle. We hypothesize that Pcs1p plays a role in the degradation of certain potentially nuclear component(s) in a manner that specifically is required for SPB duplication.

Selective proteolysis is a fundamental mechanism in the regulation of numerous biological processes (13, 42). Since protein degradation is both rapid and irreversible, it provides an effective mechanism for switching between alternative states of cellular behavior: when regulatory molecules that are required for maintenance of one state are selectively degraded, the cell switches to the second state. Such regulation has been implicated in the adaptation of plants to photosynthetic light (87), developmental decisions in *Drosophila* (46, 71), transcriptional control in yeast (22, 43, 44) and vertebrate cells (73, 94), signal transduction in yeast (54, 64), and antigen presentation in mammals (24, 79). Similarly, selective proteolysis is an essential aspect of cell cycle regulation (67), where timely progression from one stage to the next must be tightly controlled. Clearly, it is of broad importance to understand the mechanisms that mediate and regulate selective protein degradation.

In eukaryotic cells, specific proteolysis is mediated by the ubiquitin pathway (13, 34, 50), in which the covalent attachment of ubiquitin to substrate proteins targets them for degradation. Ubiquitin is activated by an E1 enzyme and then transferred by an E2 enzyme to the ubiquitin-protein ligase, E3, which catalyzes the formation of a covalent bond between ubiquitin and the protein substrate. The ubiquitin moeity then acts as a substrate for further rounds of this process, resulting in the synthesis of a poly-ubiquitin chain. The presence within cells of families of E2 and E3 enzymes that differ in their properties suggests differences in their substrate specificity. E3 enzymes are known, in fact, to play key roles in substrate selection (see below). Additionally, members of a large family of deubiquitination enzymes that have been identified are presumed to confer further regulation on the population of ubiquitinated substrates (42).

Poly-ubiquitinated proteins are degraded by proteasomes (33, 41, 75; for exceptions see 40), which are distributed throughout both the cytoplasm and the nucleus of eukaryotic cells (76). Each 26S proteasome is assembled in an ATP-dependent manner (28, 63) from a cylindrical 20S core and two 19S complexes that cap the ends of the cylinder (75) (Fig. 1). The x-ray crystal structure of the 20S complex from the archaebacterium *Thermoplasma acidophilum* was recently determined (60). This complex, which EM reveals to be structurally similar to the eukaryotic 20S particle (78), was shown to consist of four stacked ring

Please address all correspondence to Breck Byers, Department of Genetics, Box 357360, University of Washington, Seattle, WA 98195. Tel.: (206) 543-9068/1870. Fax: (206) 543-0754. e-mail: byers@genetics.washington.edu

structures. In *T. acidophilum*, each of the two outer rings consists of seven identical α subunits, while each of the inner rings consists of seven identical β subunits. Each β subunit has a proteolytic site facing the interior of the 20S cylinder, effectively sequestering its activity away from proteins that lie outside the cylinder. In eukaryotes, the rings are formed of nonidentical but related subunits. Seven related α subunit– and seven related β subunit–encoding genes have been identified in *S. cerevisiae* (41), suggesting that each ring might contain seven different subunits. It is likely that all 20S proteasomal cores in *S. cerevisiae* are identical, each one containing all 14 distinct α and β subunits (11).

Unlike the 20S proteolytic core, the structure and function of the 19S cap complex is less well understood. The 19S cap is believed to confer both specificity toward ubiquitinated substrates and an ATP dependence on proteolysis (42). Isolated mammalian 19S complexes appear to contain ~20 distinct subunits (17, 18). One subunit has been shown to bind ubiquitin polymers (19), while at least six others are members of a recently described family of ATPases (17). The 20S complex can hydrolyze proteins in the absence of ATP if the proteins are first denatured (20), suggesting that the ATPase activities of the 19S cap serve to unfold these proteins. Isopeptidase activities, which remove ubiquitin from conjugated substrates, are also associated with the 26S proteasome (13). Taken together, these observations suggest a pathway for 26S proteasome function: briefly, the 19S complex first binds a poly-ubiquitinated substrate, which then experiences ATP-dependent unfolding and translocation into the interior of the 20S cylinder, where it is hydrolyzed into small peptides. During this process, the ubiquitin chains are removed intact and recycled (50).

Ubiquitin-mediated proteolysis plays a major role in the control of cell cycle progression. The cell cycle is largely driven by the action of cyclin-dependent kinases (CDKs),[1] which are successively activated by association with cyclins (70). It has been shown, for example, that entry into mitosis requires the activity of a CDK–cyclin B complex and that completion of mitosis then requires cyclin destruction (68). Mitotic cyclins made indestructible by mutation cause arrest in mitosis, preventing the subsequent processes of chromosome decondensation, spindle disassembly, and cytokinesis (27, 30, 32, 61, 68). The temporal specificity of mitotic cyclin degradation appears to be controlled by the activity of a large ubiquitin ligase (E3) complex that is activated during mitosis (39, 90). This structure, termed the anaphase promoting complex (APC), contains *CDC16*, *CDC23*, and *CDC27* gene products in *S. cerevisiae* and their homologs in other eukaryotes (48, 52, 59, 96), as well as a homolog of the *Aspergillus nidulans* BIME product (77, 105).

Although cyclin B destruction is required for exit from mitosis, the initiation of anaphase can occur independently of cyclin B degradation (45, 91). Nevertheless, the onset of anaphase A, which is marked by sister chromatid separation, is slowed by inhibitors of the degradation machinery (45). This observation suggests that proteins other than cyclins must be degraded and that these may include those that hold sister chromatids together. Furthermore, the APC is required for progression past metaphase, as well as for exit from mitosis (48, 52, 96), indicating that this complex is also used to ubiquitinate regulatory molecule(s) whose destruction is required for the initiation of anaphase. Recent work also implicates the *S. cerevisiae PDS1* gene product as an inhibitor of sister chromatid separation that is inactivated by APC-mediated degradation (14, 103, 104). Similarly, the APC-dependent proteolysis of the *Schizosaccharomyces pombe* Cut2 protein at anaphase is essential for sister chromatid separation (26), and the *pimples* product of *Drosophila* is required for sister centromere cohesion and is rapidly degraded in mitosis (89). Besides sister chromatid separation, other aspects of spindle mechanics may also be regulated by proteolysis. For example, the *S. cerevisiae ASE1* product localizes to the spindle midzone, functions in the process of spindle elongation, and is degraded as cells exit mitosis (74), as is human CENP-E, a spindle-associated kinesin-like protein (6). Thus, proteolysis plays a fundamental regulatory role in numerous aspects of mitosis.

The effectiveness of proteolysis as a regulatory mechanism obviously depends upon the accurate and specific selection of targets for degradation. While one level of control clearly resides in specificity of substrate targeting by the APC and other ubiquitination complexes (for review see 53), further specificity might well be conferred by the proteasome itself. For example, different substrates targeted for degradation might be recognized by different subunits in the 19S cap. In this paper we report the characterization of a gene, *PCS1*, from *S. cerevisiae* that encodes a protein with extensive similarity to other subunits of the 19S cap structure. A conditional *pcs1* mutant displays a phenotype (reported here) that is distinct from those

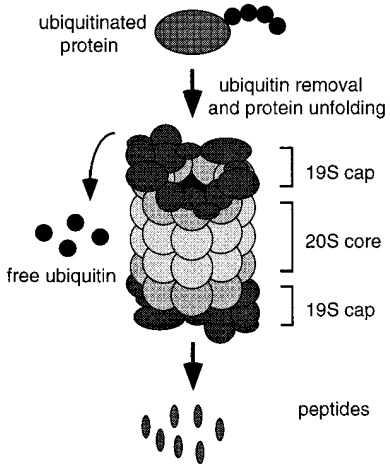

Figure 1. Schematic representation of a 26S proteasome. The 20S proteolytic barrel structure is indicated in pale grey and the 19S cap structures at either end are in dark grey. The caps are believed to recognize ubiquitinated proteins, unfold them, and feed them into the proteolytic core in an ATP-dependent manner, resulting in the release of peptides and free ubiquitin.

1. *Abbreviations used in this paper*: APC, anaphase promoting complex; CDK, cyclin-dependent kinase; DAPI, 4′,6-diamidino-2-phenylindole; 5-FOA, 5-fluoroorotic acid; GFP, green fluorescent protein; HA, hemagglutinin; SPB, spindle pole body.

caused by mutations reported for other 19S cap subunits (31). Whereas *cim3-1* and *cim5-1* mutants arrest the cell cycle at a stage with a complete spindle, EM of the present *pcs1* allele reveals a defect in duplication of the spindle pole body (SPB), which serves as the centrosome equivalent that organizes microtubule arrays in yeast (7). Before mitosis, the single SPB that is present at the beginning of the cell cycle must duplicate once (and only once) to generate the two poles of the mitotic spindle. By EM, the SPB appears as a darkly staining trilaminar disk embedded in the nuclear envelope, such that microtubules emanating from the outer and inner surfaces extend into the cytoplasmic and nuclear compartments, respectively (7). The first visible sign of SPB duplication occurs early in G1, when a small aggregate of material, termed the satellite, appears on the cytoplasmic face of the half-bridge, a darkly staining region of the envelope adjacent to the SPB. Later in G1, the satellite is transformed into a second, mature SPB that is fully embedded in the nuclear envelope. We show here that SPB duplication fails in *pcs1* cells, while other landmarks of cell cycle initiation, including bud formation and DNA replication, proceed successfully. Accordingly, we posit that *PCS1*-dependent proteolysis of specific substrate(s) is required for SPB duplication to occur.

Materials and Methods

Strains and Culture Techniques

Standard yeast genetic methods were used (66) and yeast media were made as described (37). For temperature shift experiments requiring cell synchronization, cells were arrested with 10 μM α-factor (Sigma Chemical Co., St. Louis, MO) and released as described (101). Yeast strains are listed in Table I. Bacterial strain DH5α was used for plasmid construction and bacterial media were made as described (84).

Identification and Sequence Analysis of PCS1

PCS1 was fortuitously identified during studies of *CDC31* (4). A plasmid (pHM27) encoding a lexA DNA-binding domain–Cdc31 protein fusion was used as "bait" in a two-hybrid screen (12). The L40 reporter strain (98) was cotransformed with pHM27 and the pGAD libraries (12). Library plasmids were recovered from transformants giving positive signals in the screen. A fragment of *PCS1* was found immediately downstream from the *GAL4* activation domain sequence in one plasmid, YL2-29, but subcloning showed that a gene elsewhere in the genomic DNA insert (*CDC31*) was responsible for the signal. Independent library plasmids containing *CDC31* were identified, mapped, and shown to contain *PCS1* in the same relative position. One plasmid, YL1-19, contained the complete *PCS1* sequence.

The *PCS1* gene was sequenced on both strands using YL2-29, YL1-19, and constructs derived from these plasmids as templates. Sequencing reactions were done using the Taq DyeDeoxy terminator cycle sequencing kit (Applied Biosystems, Foster City, CA) and were analyzed by the University of Washington Molecular Pharmacology Facility using an Applied Biosystems 373A automated sequencer. Oligonucleotides designed to prime the sequencing reactions at appropriate positions in *PCS1* were synthesized by GIBCO BRL (Gaithersburg, MD). Sequence assembly and analysis were performed using the Genetics Computer Group package (36), and comparisons with sequence databases were performed using the BLAST program (2).

Genomic Disruption of PCS1

As a first step toward disrupting *PCS1*, the yeast integrating plasmids pHM35 and pHM47 were constructed. Standard recombinant DNA techniques were used (84), and restriction enzymes, DNA polymerases, and T4 DNA ligase were purchased from New England Biolabs (Beverly, MA). To introduce a unique EcoRI site in the region of the gene encoding the ATPase domain, oligonucleotide primers hm15-BamHI (5′GAAGATCTCGGATCCACTGGTG3′) and hm16-EcoRI (5′GGAATTCTATAACCTCCCTTAA3′) (underlined nucleotides represent restriction sites) were used together with Vent™ DNA polymerase (New England Biolabs) to amplify YL2-29 template DNA between nucleotides 583 and 689 (see Fig. 2 *B*) in a PCR. The product was digested with BamHI and EcoRI and ligated into BamHI/EcoRI-digested pRS306 (88) to create plasmid pHM34. Primers hm17-EcoRI (5′CGAATTCCCATTGAAGAACCCAG3′) and hm18-KpnI (5′CCGGTACCAGGGGGAC3′) were used to amplify the YL2-29 template between nucleotides 685 and 775. This product was digested with EcoRI and KpnI and ligated into EcoRI/KpnI-digested pHM34 to create pHM35. The insert in pHM35 was excised with BamHI and KpnI and ligated into BamHI/KpnI-digested pRS304 (88) to create pHM47.

To disrupt one genomic copy of *PCS1*, plasmid pHM47, which carries the *TRP1* gene, was digested with EcoRI and used to transform the diploid yeast strain D8bx5cA (which is congenic with S288C) to Trp^+. Southern blot analysis (not shown) confirmed that integration of pHM47 into one copy of *PCS1* had occurred as expected in the transformant used in further experiments (YHM9.1).

Construction of a Temperature-sensitive PCS1 Allele

To create a temperature-sensitive *PCS1* mutant, we constructed plasmid pHM55, which encodes a degron–Pcs1p fusion. The EcoRI–HindIII fragment encoding the degron unit (Ub-$DHFR^{ts}$-ha) (21) was previously cloned into the EcoRI–HindIII sites in the pRS316 polylinker by Dr. Frank Russo (University of Washington, Seattle, WA). This fragment was excised with EcoRI and ClaI and treated with Klenow. pHM53 (see below) was digested with NcoI and treated with Klenow, and the degron-encoding fragment was ligated into this site. These manipulations resulted in the degron fragment being inserted at the start codon of *PCS1*, in frame with the open reading frame. We refer to this allele as $pcs1^{td}$ (temperature-inducible degron allele). Next, the yeast integrating plasmid pHM56

Table I. Saccharomyces cerevisiae Strains

Strain	Genotype	Source
D8bx5cA	*MAT**a**/MATα, ura3-52/ura3-52, trp1Δ/trp1Δ, leu2-3,112/leu2-3,112, his3Δ/his3Δ*	M. Winey
YHM9.1	*MAT**a**/MATα, ura3-52/ura3-52, trp1Δ/trp1Δ, leu2-3,112/leu2-3,112, his3Δ/his3Δ, pcs1::TRP1/PCS1*	This study
YHM10.1.49	*MAT**a**, ura3-52, leu2-3,112, trp1Δ, his3Δ, pcs1::TRP1* [pHM49: *PCS1* on pRS316 *(CEN-URA3)*]	This study
YHM10.1.54	*MAT**a**, ura3-52, leu2-3,112, trp1Δ, his3Δ, pcs1::TRP1* [pHM54: *GFP-PCS1* on pRS315 *(CEN-LEU2)*]	This study
Wx257-5c	*MAT**a**, ura3-52, leu2-3,112, trp1Δ, his3Δ*	M. Winey
YHM11.2	*MAT**a**, ura3-52, leu2-3,112, trp1Δ, his3Δ,* $pcs1^{td}$	This study
YHM12.1	*MAT**a**, ura3-52, leu2-3,112, trp1Δ, his3Δ,* $pcs1^{td}$*, ubr1Δ::HIS3*	This study
YHM13.1	*MAT**a**, ura3-52, leu2-3,112, trp1Δ, his3Δ, ubr1Δ::HIS3*	This study
CMY763	*MATα, ura3-52, leu2Δ1, his3Δ-200, cim3-1*	C. Mann
CMY765	*MATα, ura3-52, leu2Δ1, his3Δ-200, cim5-1*	C. Mann
MHY849	*MATα, sen3::TRP1 (YEplac195SEN3), his3Δ-200, leu2-3,112, ura3-52, lys2-801*	M. Hochstrasser
MHY851	*MATα, sen3::TRP1 (YEplac195SEN3ha), his3Δ-200, leu2-3,112, ura3-52, lys2-801*	M. Hochstrasser

was constructed. The insert from pHM55 was excised with PvuII and inserted into PvuII-digested pRS306 (88) to create pHM56.

To replace the wild-type *PCS1* gene with the *pcs1^{td}* allele in the chromosome, the two-step "pop-in/pop-out" gene replacement method was used (81, 85). pHM56 was digested with EcoRI and used to transform the haploid strain Wx257-5c (which is congenic with S288C) to Ura$^+$. PCR analysis confirmed that integration had occurred at the *PCS1* locus as predicted (data not shown), resulting in both *PCS1* and *pcs1^{td}* flanking the plasmid sequences. Excision of the plasmid and either of the *PCS1* alleles via homologous recombination was then selected for using 5-fluoroorotic acid (5-FOA; PCR Inc., Gainesville, FL), which kills Ura3$^+$ cells (5). Two 5-FOA–resistant colonies were identified that had a temperature-sensitive phenotype, suggesting that they contained the *pcs1^{td}* allele. PCR analysis confirmed that this was true in the *pcs1^{td}* strain used in further experiments, YHM11.2 (data not shown).

To delete *UBR1* from both YHM11.2 and Wx257-5c, plasmid pJDubrΔ4-B (a gift from Drs. Jürgen Dohmen and Alexander Varshavsky, California Institute of Technology, Pasadena) was digested with EcoRI and used to transform these yeast strains to His$^+$. This manipulation resulted in the replacement of *UBR1* with the *ubr1Δ::HIS3* allele, creating strains YHM12.1 (*pcs1^{td}*) and YHM13.1 (*PCS1*).

Plasmid Constructions

Plasmids pHM48 and pHM49 were constructed to supply *PCS1* function in a haploid yeast strain containing a disrupted genomic copy of *PCS1*. Primers hm27-XhoI (5′CCGCTCGAGAAGCTTGAAATACCATAGTG3′) and hm28-SmaI (5′TCCCCCGGGAGTTCAATAGCCATTTCGAGC3′) were used together with Vent^{TM} DNA polymerase to amplify the YL1-19 template between nucleotides 1 and 1,506 (Fig. 2 *B*). The product was digested with XhoI and SmaI and ligated into the yeast centromere (*CEN*) plasmids pRS315 and pRS316 (88), also digested with XhoI and SmaI, to create plasmids pHM48 and pHM49.

To facilitate later constructions, a unique NcoI site was engineered to overlap the *PCS1* start codon in pHM48. Primer hm32-NcoI (5′CCTGTTCTTCACCCATGGTTAGTTATTAATATCTTTG3′) was used in a PCR-based site-directed mutagenesis technique (10). Primers hm32-NcoI and T3 (whose site is outside the polylinker upstream from the *PCS1* gene in pHM48) were used to amplify a fragment of DNA from pHM48. This fragment was then used as a primer, together with the T7 primer (whose site is outside the polylinker downstream from the *PCS1* gene in pHM48) in a second PCR. The second PCR product was digested with XhoI and SstI and ligated into XhoI/SstI-digested pRS315 (88) to create plasmid pHM53. As a result of the site-directed mutagenesis, the second codon in *PCS1* was changed from AGT (Ser) to GGT (Gly).

Plasmid pHM54 was constructed to encode a green fluorescent protein (GFP)–Pcs1 protein fusion. Plasmid pZA66 was previously constructed by Dr. Michael Moser (University of Washington). It encodes S65T GFP (38) engineered to contain a COOH-terminal 10–amino acid spacer consisting of repeating Gly-Ala residues. The DNA fragment encoding this unit was excised from pZA66 with BspHI and ligated into NcoI-digested pHM53 to create pHM54. This manipulation resulted in the S65T GFP encoding DNA being inserted in frame with the *PCS1* gene, at the *PCS1* start codon.

Cytological Techniques and Protein Analysis

Cells were prepared for immunofluorescence microscopy as described (49, 51). To detect microtubules, the rat monoclonal anti–α-tubulin antibody YOL1/34 (Accurate Chemical and Scientific Corp., Westbury, NY) and FITC-conjugated goat anti–rat antibodies (Amersham Corp., Arlington Heights, IL) were used at dilutions of 1:100 and 1:50, respectively. For hemagglutinin (HA) epitope tag localization, mAb 12CA5 (Boehringer Mannheim Biochemicals, Indianapolis, IN) was used at a concentration of 0.8 μg/ml followed by FITC-conjugated goat anti–mouse antibodies (Amersham Corp.) diluted 1:100. DNA was visualized with 4′,6-diamidino-2-phenylindole (DAPI) (1 μg/ml; Sigma Chemical Co.). Fixed and stained cells were viewed using a Microphot FX fluorescent microscope (Nikon Inc., Garden City, NY) and photographed with TMAX 400 film (Eastman Kodak Co., Rochester, NY).

Cells containing the GFP–Pcs1p fusion were grown to a density of ~10^7 cells per ml and stained with DAPI by first resuspending the cells briefly in methanol, washing with PBS, and resuspending in a 1 μg/ml DAPI solution. These cells were viewed and photographed as described above.

Yeast cells were prepared for thin-section EM as described (9). Serial sections were viewed on an EM300 electron microscope (Philips Electronic Instruments, Inc., Mahwah, NJ).

Cells were prepared for flow cytometry as described (47). Propidium iodide (Sigma Chemical Co.) was used to stain the DNA. A Becton Dickinson FACS®can flow cytometer (San Jose, CA) was used together with the CELLFIT and LYSYS software packages.

For Western blot analysis, whole cell lysates were prepared from yeast spheroplasts as follows. Spheroplasts derived from 5-ml cultures at a density of 3×10^7 cells per ml were resuspended in 100 μl lysis buffer (50 mM Tris-Cl, pH 7.5, 1 mM EDTA, 1 mM DTT, 1 mM PMSF, 0.5 μg/ml leupeptin, 2 μg/ml aprotinin) and lysed using 20 strokes in a Dounce homogenizer. This solution was centrifuged for 15 min at top speed in a microfuge at 4°C, and the supernatant was transferred to a fresh tube. Total protein concentration in the clarified lysates was determined using the Bio-Rad protein assay (Bio Rad Laboratories, Hercules, CA) and BSA as a standard. Equivalent amounts of total protein were subjected to SDS-PAGE (58). Proteins were transferred to nitrocellulose in a transphor electrophoresis unit (Hoefer Scientific Instruments, San Francisco, CA) for 1 h at 0.3 A. The nitrocellulose membrane was blocked with 5% nonfat dry milk in TBS/Tw (TBS, 0.05% Tween-20) for 1 h, and then incubated with anti-GFP antiserum (Clontech, Palo Alto, CA) at a 1:4,000 dilution in TBS/Tw for 1 h. The membrane was washed in TBS/Tw and incubated with goat anti–rabbit IgG-HRP (Accurate Chemical and Scientific Corp.) at a 1:5,000 dilution for 1 h, followed by washing in TBS/Tw. All incubations were done at room temperature. The signal was developed using the enhanced chemiluminescence system (Amersham Corp.).

Results

Identification and Sequence Analysis of PCS1

We identified *PCS1* while sequencing near *CDC31* (4), a gene located on the right arm of *S. cerevisiae* chromosome XV (see Materials and Methods for experimental details and rationale). Briefly, one end of a genomic fragment of DNA containing *CDC31* internally was sequenced and found to encode a portion of a novel gene encoding a new member of a diverse family of ATPases (86). Since members of this family are known to play roles in the regulation of mitosis, we pursued its characterization further. We identified a plasmid (YL1-19) containing an 11-kb insert that includes the full-length version of the new gene. It is located ~1 kb from *CDC31* and faces in the opposite orientation. A partial restriction map of the relevant portion of the YL1-19 insert is shown in Fig. 2 *A*; the relative positions of *PCS1*, *CDC31*, and a third open reading frame are indicated by arrows beneath the map. Sequence analysis revealed that a 1.3-kb open reading frame (Fig. 2 *B*), designated *PCS1*, represents the novel ATPase-encoding gene.

To examine the relationship between Pcs1p and other protein sequences in the databases, we used the BLAST alignment program (2). This analysis confirmed the identity of Pcs1p as a member of the "AAA" (ATPases Associated with diverse cellular Activities [56]) superfamily. Members of this superfamily share a conserved region of ~200 amino acids that contains motifs A and B characteristic of ATP binding, underlined in Fig. 2 *B* (99). Pcs1p is most similar to a subclass of this superfamily composed of proteasomal 19S cap subunits. Fig. 3 shows an alignment of Pcs1p with three of the highest scoring proteins in the BLAST search. p42 (25) and S4 (23) are subunits of the human 26S proteasome, and their sequences are respectively 67% and 38% identical to the Pcs1p sequence as determined by the pairwise alignment program BESTFIT (36). *SUG1* (92)/*CIM3* (31) (and *CIM5* [31]) are *S. cerevisiae* genes; the sequences of their predicted products are 43% and 39% identical to the Pcs1p sequence. Homologs of the *SUG1*/*CIM3* and *CIM5* gene products were identi-

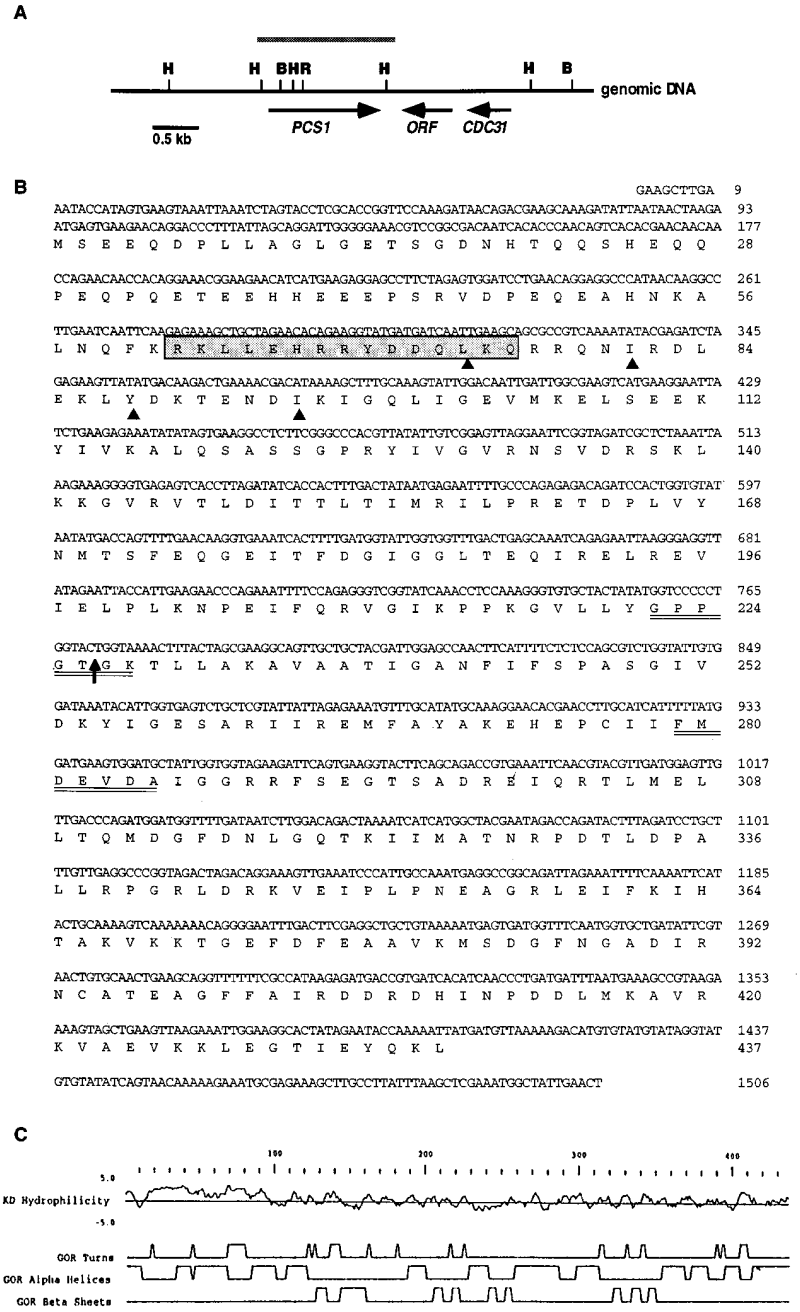

Figure 2. Organization and sequence analysis of the *PCS1* gene. (*A*) Partial restriction map of the genomic region surrounding *PCS1*. The *PCS1* and *CDC31* coding regions are indicated by arrows beneath the map; *ORF* indicates a third open reading frame. The line above the map represents the sequenced region shown in *B*; this region is sufficient to supply *PCS1* function in cells lacking other functional copies of the gene. *H*, HindIII; *B*, BamHI; *R*, EcoRI. (*B*) Nucleotide and predicted amino acid sequence of *PCS1*. A potential nuclear localization signal is boxed; a heptad repeat characteristic of α-helical coiled-coils is indicated by triangles; sequence motifs characteristic of an ATP-binding domain are underlined; and the site of gene disruption described in the text is indicated by an arrow under the first ATP motif. These sequence data are available from GenBank/EMBL/DDBJ under accession number U93262. The *PCS1* sequence is also entered in these databases as *SUG2* (accession number SCU43720 [GB]) (83) and in the *S. cerevisiae* genome database by J.H. McCusker (Duke University Medical Center, Durham, NC) and J.E. Haber (Brandeis University, Waltham, MA) as representing *CRL13*, which was originally identified by a temperature-sensitive, cycloheximide-resistant allele (65). (*C*) Structural analysis of Pcs1p. The top line is a graphical representation of the relative hydrophilicity of its amino acid sequence (57). The next three lines represent secondary structural predictions calculated by the method of Garnier et al. (29) and displayed in graphical form. Regions predicted to form turns, α helices, or β sheets are indicated by elevation of the appropriate line.

fied in purified preparations of 26S proteasomes from *Drosophila* (31), and the Sug1/Cim3 protein has been directly shown to be a subunit of the yeast 26S proteasome (82). Pcs1p is also closely related to the *S. pombe mts2*$^+$ gene product, a 26S proteasome component necessary for completion of mitosis (35). The very high degree of sequence similarity between these known proteasome cap subunits and Pcs1p provides strong evidence that Pcs1p is itself a 19S cap subunit. This identity has been confirmed by the recent work of Russell et al. (83), who demonstrated that the protein encoded by *SUG2* (which is identical to *PCS1*) is a component of the 26S proteasome, while our work was in progress.

PCS1 is predicted to encode a protein 437 amino acids in length, with an expected molecular mass of 49 kD and isoelectric point of 5.5. A notable characteristic of Pcs1p is the very hydrophilic region extending between amino acids 13 and 96, shown graphically in Fig. 2 *C*. This region also corresponds to the most divergent part of Pcs1p compared with the sequences most closely related to it (Fig. 3). Additionally, the boxed region indicated in Fig. 2 *B* is predicted to be a potential nuclear localization signal by the program PSORT (69). To gain further information about the conformation of Pcs1p, we used the method of Robson-Garnier (29) to predict the secondary structural features of the Pcs1p sequence. This analysis, also depicted graphically in Fig. 2 *C*, suggests that the protein may be largely globular, since the three conformational features of

α helix, turn, and β sheet generally alternate. One region largely predicted to be α-helical, between amino acid residues 74 and 101, displays a limited heptad repeat motif suggestive of the ability to form a short α-helical coiled-coil. This motif consists of a repeating heptad with hydrophobic residues enriched at positions 1 and 4 (1) (residues at position 1 are indicated with a triangle beneath them in Fig. 2 *B*). The program COILS (62) gives this region a probability near 1.0 of adopting a coiled-coil conformation. Other members of the 19S ATPase family also contain heptad motifs near their NH_2 termini (78).

PCS1 Is Essential for Vegetative Growth

To determine whether *PCS1* gene function is essential for cell viability, we constructed haploid strains disrupted for *PCS1* (*pcs1*::*TRP1*). We reasoned that the highly conserved ATP-binding motif A (P-loop; underlined in Fig. 2 *B*) would almost certainly be essential for Pcs1p function. Therefore, we constructed a plasmid, pHM47, that when integrated into the genome results in the insertion of the *S. cerevisiae TRP1* gene into the P-loop–encoding region (see Materials and Methods); the insertion site is indicated by the arrow in Fig. 2 *B*. The diploid strain D8bx5cA was transformed with this plasmid, which was cut at EcoRI to direct integration at the *PCS1* locus. Southern blotting was used to confirm that the plasmid had integrated into one copy of *PCS1* as expected in each of eight Trp^+ transformants (data not shown). The transformant chosen for further experiments (designated YHM9.1) was sporulated, and the resulting tetrads were dissected. In all cases (20/20), the four spores segregated in a ratio of two viable to two inviable; this result held true at both 23° and 37°C. The viable spores were always auxotrophic for tryptophan, indicating that they did not carry the disruption marker. We examined the phenotype of the inviable spore microcolonies after 3 d at either 23° or 37°C and observed a small effect of temperature on the cell cycle at which division arrested. At 23°C, the spore germinated and divided twice, arresting as four large-budded cells. At 37°C, the spore germinated and divided once, arresting in the second division cycle as two large-budded cells. Often the bud was misshapen and could not be pulled away from the mother cell with a dissecting needle. These results indicate that *PCS1* function is necessary for cell viability and are consistent with an essential role for this protein in mitosis.

To determine whether the sequenced length of DNA shown in Fig. 2 *B* is sufficient to supply *PCS1* function, we constructed a plasmid (pHM49; see Materials and Methods) that contains the *PCS1* sequence carried on a *CEN*-based vector marked with *URA3.* pHM49 was transformed into strain YHM9.1, which is heterozygous for the *pcs1*:: *TRP1* disruption. Sporulation and tetrad analysis revealed that more than two spores per tetrad formed colonies. All

```
Pcs1      1 ......MSEEQDPLLAGLGETSGDNHTQQSHEQQPEQPQETEEHHEEEPSRVDPEQEAHN
p42       1 ..........................................................MADPRD
Cim3      1 ..........................................MTAAVTSSNIVLETH..ESGI
S4        1 MGQSQSGGHGPGGGKKDDEDKKKKYEPPVPTRVGKKKKKRKGPDAASKLPLVTPHTQCRL

Pcs1     55 KAL..NQFKRKLLEHRRYDDQLKQRRQNIRDLEKLYDKTENDIKALQSIGQLIGEVMKEL
p42       7 KAL..QDYRKKLLEHKEIDGRLKELREQLKELTKQYEKSENDLKALQSVGQIVGEVLKQL
Cim3     20 KPYFEQKIQETELKIRSKTENGRRLEAQRNALNDKVRFIKDELRLLQEPGSYVGEVIKIV
S4       61 KLLKLERIKDYLL....MEEEFIRNQEQMKPLEEKQEEERSKVDDLRGTPMSVGTLEEII

Pcs1    113 SEEKYIVKASSGPRYIVGVRNSVDRSKLKKGVRVTLDITTLTIMRILPRETDPLVYNMTS
p42      65 TEEKFIVKATNGPRYVVGCRRQLDKSKLKPGTRVALDMTTLTIMRYLPREVDPLVYNMSH
Cim3     80 SDKKVLVKVQPEGKYIVDVAKDINVKDLKASQRVCLRSDSYMLHKVLENKADPLVSLMMV
S4      117 DDNHAIVSTSVGSEHYVSILSFVDKDLLEPGCSVLLNHKVHAVIGVLMDDTDPLVTVMKV

Pcs1    173 FEQGEITFDGIGGLTEQIRELREVIELPLKNPEIFQRVGIKPPKGVLLYGPPGTGKTLLA
p42     125 EDPGNVSYSEIGGLSEQIRELREVIELPLTNPELFQRVGIIPPKGCLLYGPPGTGKTLLA
Cim3    140 EKVPDSTYDMVGGLTKQIKEIKEVIELPVKHPELFESLGIAQPKGVLLYGPPGTGKTLLA
S4      177 EKAPQETYADIGGLDNQIQEIKESVELPLTHPEYYEEMGIKPPKGVILYGPPGTGKTLLA

Pcs1    233 KAVAATIGANFIFSPASGIVDKYIGESARIIREMFAYAKEHEPCIIFMDEVDAIGGRRFS
p42     185 RAVASQLDCNFLKVVSSSIVDKYIGESARLIREMFNYARDHQPCIIFMDEIDAIGGRRFS
Cim3    200 RAVAHHTDCKFIRVSGAELVQKYIGEGSRMVRELFVMAREHAPSIIFMDEIDSIGSTRVE
S4      237 KAVANQTSATFLRVVGSELIQKYLGDGPKLVRELFRVAEEHAPSIVFIDEIDAIGTKRYD

Pcs1    293 EGTSADREIQRTLMELLTQMDGFDNLGQTKIIMATNRPDTLDPALLRPGRLDRKVEIPLP
p42     245 EGTSADREIQRTLMELLNQMDGFDTLHRVKMTMATNRPDTLDPALLRPGRLDRKIHIDLP
Cim3    260 GSGGGDSEVQRTMLELLNQLDGFETSKNIKIIMATNRLDILDPALLRPGRIDRKIEFPPP
S4      297 SNSGGEREIQRTMLELLNQLDGFDSRGDVKVIMATNRIETLDPALIRPGRIDRKIEFPLP

Pcs1    353 NEAGRLEIFKIHTAKVKKTGEFDFEAAVKMSDGFNGADIRNCATEAGFFAIRDDRDHINP
p42     305 NEQARLDILKIHAGPITKHGEIDYEAIVKLSDGFNGADLRNVCTEAGMFAIRADHDFVVQ
Cim3    320 SVAARAEILRIHSRKMNLTRGINLRKVAEKMNGCSGADVKGVCTEAGMYALRERRIHVTQ
S4      357 DEKTKKRIFQIHTSRMTLADDVTLDDLIMAKDDLSGADIKAICTEAGLMALRERRMKVTN

Pcs1    413 DDLMKAVRKVAEVKKLEGTIEYQKL..
p42     365 EDFMKAVRKVADSKKLESKLDYKPV..
Cim3    380 EDFELAVGKVMN.KNQETAISVAKLFK
S4      417 EDFKKSKENVLY.KKQEGTPEGLYL..
```

Figure 3. Multiple sequence alignment of Pcs1p, p42, Sug1/Cim3 protein, and S4. (*Black boxes*) Amino acid identity; (*grey boxes*) similarity. This display was created using the program BOXSHADE.

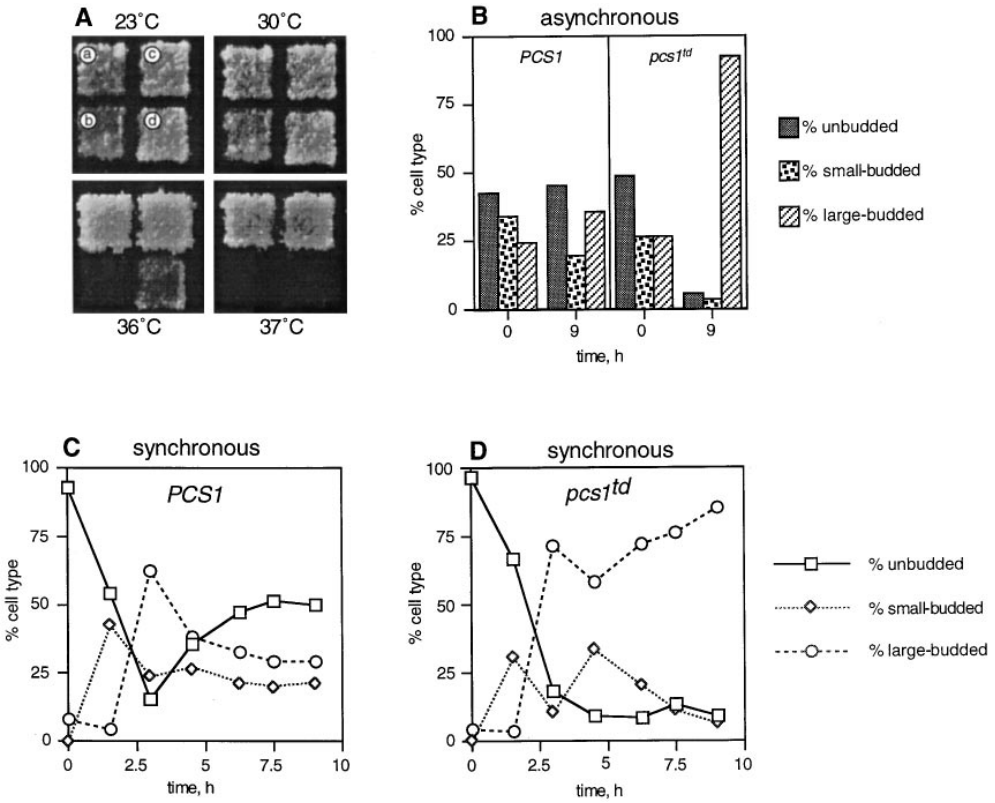

Figure 4. Characterization of *pcs1^{td}*. (*A*) Growth at different temperatures of yeast strains containing *PCS1* or *pcs1^{td}*. Each panel represents duplicate patches of the following yeast strains: (*a*) Wx257-5c (*PCS1*), (*b*) YHM11.2 (*pcs1^{td}*), (*c*) YHM13.1 (*PCS1*, *ubr1Δ::HIS3*), and (*d*) YHM12.1 (*pcs1^{td}*, *ubr1Δ::HIS3*). (*B*) Percentages of unbudded, small-budded, and large-budded cells in asynchronous *PCS1* and *pcs1^{td}* strains before and after shift to 37°C. (*C* and *D*) Percentages of cell types in synchronous *PCS1* and *pcs1^{td}* strains. A shift from 23° to 37°C occurred at time 0.

Trp$^+$ colonies were also Ura$^+$, indicating that a haploid strain disrupted for chromosomal *PCS1* can be maintained by the sequence cloned in pHM49.

Construction of a Temperature-sensitive pcs1 Allele

To obtain a conditional allele that could be used for more detailed phenotypic analysis, we constructed a haploid strain, designated YHM11.2, in which the chromosomal *PCS1* gene was replaced with an allele (*pcs1^{td}*) that encodes a degron–Pcs1p fusion (see Materials and Methods). The degron unit is a heat-inducible degradation signal (21) that at high temperature (37°C) is degraded, together with sequences fused downstream of it, by the N-end rule pathway of protein degradation (3). Strain YHM11.2 was viable at 23° and 30°C (Fig. 4 *A*, patch *b*), but was inviable at 36° and 37°C. Strain Wx257-5c, the wild-type strain from which YHM11.2 is derived, was viable at all temperatures tested (Fig. 4 *A*, patch *a*). Thus, *pcs1^{td}* is a temperature-sensitive allele of *PCS1*. We also confirmed that the *pcs1^{td}* mutation is recessive, as expected for an allele designed to encode a protein that is degraded rapidly: *pcs1^{td}*/*PCS1* diploid cells grew normally at 37°C (data not shown), and the mutant phenotype caused by *pcs1^{td}* can be complemented by pHM49 (see above).

To test whether this temperature sensitivity is a result of degradation via the N-end pathway as predicted, we deleted *UBR1* from strains YHM11.2 and Wx257-5c to create strains YHM12.1 and YHM13.1, respectively. The *UBR1* gene is required for the N-end rule pathway and for the temperature sensitivity of several alleles encoding degron fusions (21). We found that deleting *UBR1* partially rescued the temperature sensitivity caused by *pcs1^{td}*. Although deletion of *UBR1* does not restore growth of the *pcs1^{td}* strain at 37°C (Fig. 4 *A*, patch *d*), growth did occur at 36°C. These results confirm an important role for the N-end rule pathway in the loss of function for *pcs1^{td}*.

pcs1^{td} Strains Arrest as Large-budded Cells with a G2 Content of DNA

To determine whether depletion of *PCS1* function causes arrest at a specific stage in the cell cycle, we shifted asynchronous liquid cultures of strains Wx257-5c (*PCS1*) and YHM11.2 (*pcs1^{td}*) from 23° to 37°C and observed their behavior after various times. Fig. 4 *B* shows the relative proportions of unbudded, small-budded, and large-budded cells after 9 h at the restrictive temperature. About 90% of the *pcs1^{td}* cells were found to be large budded at the restrictive temperature, compared with ~30% for the culture continuing to grow at the permissive temperature. To investigate the kinetics of entry into this state of arrest, we used synchronous cultures of *PCS1* and *pcs1^{td}* obtained by arresting growth in G1 with α-factor and then shifting them to 37°C in fresh media without α-factor. Fig. 4, *C* and *D*, shows the proportions of cell types at time points after this shift. From this experiment it is clear that *pcs1^{td}* cells underwent at least two cell divisions before becoming arrested as large-budded cells, since a second cycle of bud formation was evident at ~5 h. We also noted a partial defect in cell separation, for pairs of budded cells remained attached to each other as the second cell cycle progressed. By 9 h after release from α-factor, ~25% of the cells were detected as attached pairs of large-budded cells.

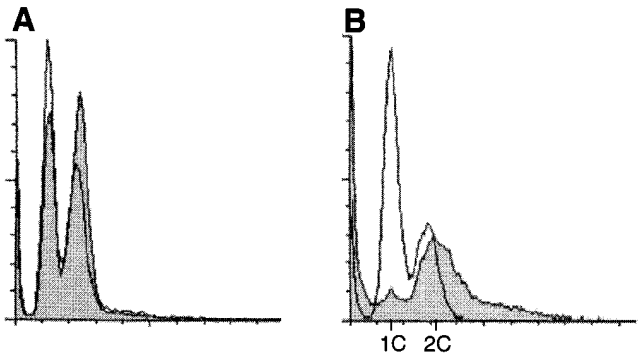

Figure 5. Flow cytometric analysis of *pcs1*^{td}. (*A*) Wx257-5c (*PCS1*, *open curve*) compared with YHM11.2 (*pcs1*^{td}, *shaded curve*) at 23°C. (*B*) *PCS1* (*open curve*) compared with *pcs1*^{td} (*shaded curve*) at 37°C. The left peak represents G1 cells and the right peak represents G2/M cells. In these histograms, the x-axis indicates relative DNA content measured by propidium iodide fluorescence, and the y-axis indicates the relative number of cells. Each sample represents 15,000 cells.

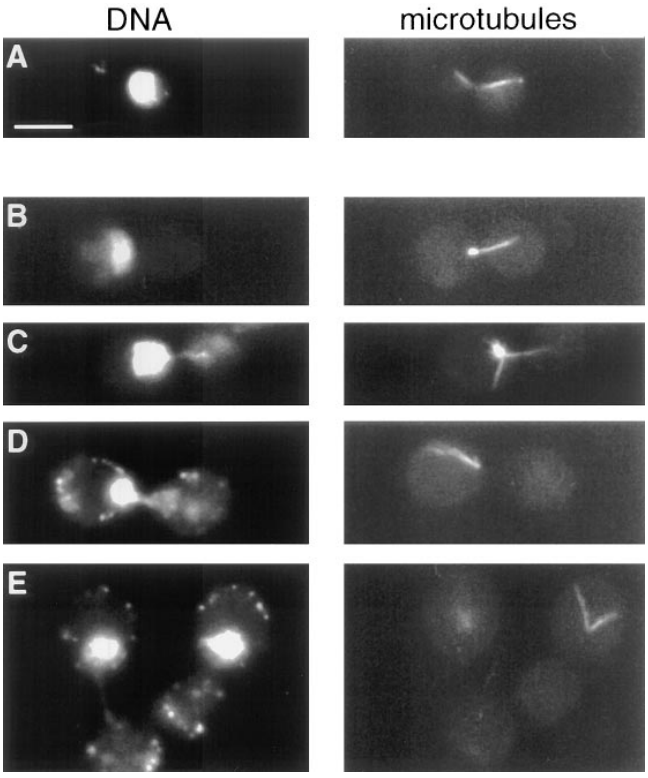

Figure 6. Cytological analysis of *pcs1*^{td} cells using immunofluorescence microscopy. (*Left*) DNA staining (DAPI); (*right*) microtubule staining (FITC). (*A*) Wx257-5c (*PCS1*) at 37°C. (*B–E*) YHM11.2 (*pcs1*^{td}) at 37°C. Intranuclear spindles appear to be absent in the mutant cells. Bar, 5 μm.

We also followed individual cells after shift to the restrictive temperature. Cells were arrested with α-factor, transferred to a plate, and observed after 27 h at 37°C. About half of the cells had arrested in the second cycle as two large-budded cells, while the other half had completed this cycle and undergone the same type of arrest in the third cycle. It has been observed that the effectiveness of the degron system improves if cells are held in stationary phase before the temperature shift (Dirick, L., personal communication). Accordingly, we permitted *pcs1*^{td} cells to remain at stationary phase for 3 d at 23°C, at which time ~90% were unbudded, transferred them to a plate, and again observed them after incubation for 27 h at 37°C. 50% of the cells reached the final stage of arrest as large-budded cells within the first cycle, 30% in the second cycle, and 20% in the third, suggesting that degron–Pcs1p was more effectively depleted in this experiment.

Flow cytometry experiments indicate that *pcs1*^{td} cells arrest with a 2C (G2) content of DNA. Fig. 5 *A* shows the cytometry profiles of asynchronous *PCS1* and *pcs1*^{td} cultures at 23°C, where it can be seen that about equal proportions of *pcs1*^{td} cells had apparent 1C and 2C DNA contents. After 9 h at 37°C, however, 87% of the *pcs1*^{td} cells had accumulated in a state with a 2C content of DNA, whereas a higher proportion of *PCS1* cells had a 1C content of DNA at 37°C than at 23°C (Fig. 5 *B*). These findings demonstrate that cells lacking *PCS1* function undergo arrest in the division cycle after DNA synthesis, and that this function therefore must be required for progression from G2 into mitosis.

PCS1 Function Is Required for Spindle Pole Body Duplication

To gain a better understanding of how a lack of *PCS1* function perturbs mitosis, we visualized DNA and microtubules using fluorescence microscopy in *pcs1*^{td} cells that had accumulated in the terminal arrest described by flow cytometry (see above). After 9 h at 37°C, the DNA remained unsegregated and was localized in a region immediately adjacent to the bud neck in ~80% of these cells (Fig. 6, *B–E*). Nuclei occupying this position in *PCS1* cells grown at 37°C were shown by tubulin antibody staining to contain a short intranuclear spindle (Fig. 6 *A*), as is characteristic of yeast cells in G2 or mitotic metaphase. However, the arrested *pcs1*^{td} cells did not contain discrete spindles and generally had fewer detectable intranuclear microtubules. The most common phenotype is shown in Fig. 6 *B*, in which a single bundle of cytoplasmic microtubules extended away from the nucleus and through the bud neck. Additionally, some cells contained a relatively bright focus of microtubule staining at the nuclear periphery, as well as cytoplasmic microtubules emanating away from this focus (Fig. 6 *C*). Less frequently, we observed cells in which microtubules appeared to lie along the surface of the nucleus (Fig. 6 *D*), and other cells in which two bundles of cytoplasmic microtubules extended away from the nucleus in an antennae-like array (Fig. 6 *E*). (Significant numbers of cells lacking spindle structures were not observed at earlier time points in this experiment, presumably because the first cycle proceeded normally, albeit slowly.) These findings suggest that cells deprived of *PCS1* function fail to form a mitotic spindle while retaining the ability to assemble cytoplasmic microtubule arrays.

The attachment between pairs of large-budded cells seen after transfer of a *pcs1*^{td} culture to the restrictive tem-

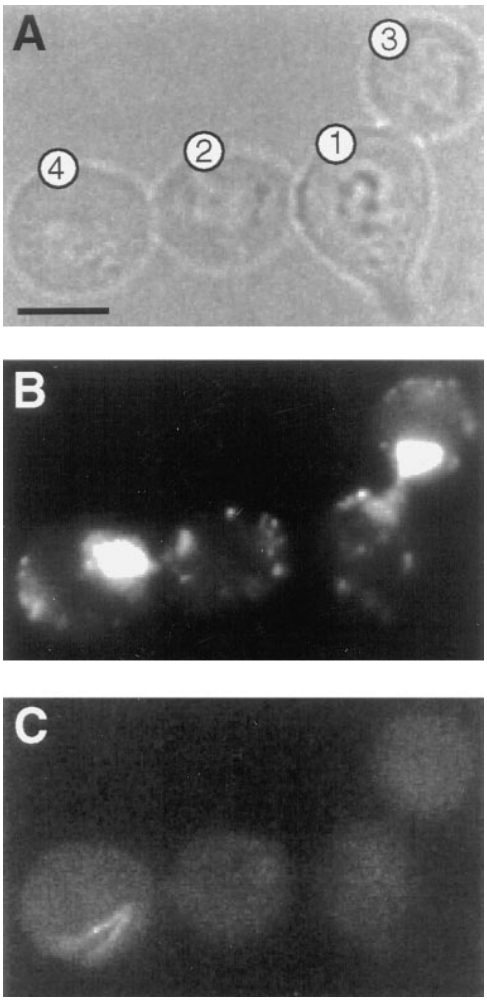

Figure 7. DNA localization in linked large-budded *pcs1*^{td} cells at 37°C. (*A*) Nomarski image of cells. The numbers designate the presumed order of budding, as explained in the text. (*B*) DNA (DAPI). (*C*) Microtubules (FITC). Bar, 5 μm.

perature (as described earlier) provided us with a method of identifying mother and daughter cells unambiguously. Fig. 7 *A* shows cells in this configuration. Since the cells had been arrested with α-factor before the shift to high temperature, the original mother is identifiable as the schmoo-shaped cell 1. This cell presumably had budded once to produce cell 2 and a second time to produce bud 3. Cell 2 had also budded to produce bud 4. In Fig. 7 *B*, it can be seen that the unsegregated DNA lies largely within the buds (3 and 4) that are the products of the second division. Cytoplasmic microtubule staining is evident in bud 4 (Fig. 7 *C*); faint microtubule staining was also observed in bud 3 in a different focal plane. Although we could not distinguish the mother cell and bud unambiguously among all cells examined in this manner, the DNA localized to the mother ~50% of the time and bud 50% of the time when both could be identified (data not shown). A mutant that is specifically defective in spindle pole body duplication, *ndc1-1*, has previously been shown to display random localization of the single functional spindle pole and the bulk of the DNA between the mother cell and the bud (93, 97). Similarly, certain mutations that cause cells to arrest with a bipolar spindle also display such random localization of DNA (72).

Given our finding that the *pcs1*^{td} cells arrest more quickly if held in stationary phase before a shift to the restrictive temperature, we also examined the microtubule arrays of cells treated in this manner at various times after the temperature shift. Since mutations in the closely related *SUG1*/*CIM3* and *CIM5* genes have previously been reported to cause cells to arrest with short spindles (31), we also wished to determine whether the phenotypes of *pcs1*^{td}, *cim3-1*, and *cim5-1* mutants were indeed distinct when the same conditions were used for the experiment. Accordingly, strains YHM11.2 (*pcs1*^{td}), CMY763 (*cim3-1*), and CMY765 (*cim5-1*) (each congenic with the S288C background) were held at stationary phase for 3 d at 23°C, and then diluted into fresh media at 37°C. At the time of the temperature shift, no abnormal spindles were observed in any of the strains. Fig. 8 shows the percentage of large-budded cells containing short spindles, long spindles, or no spindles in each of the strains at different times after the temperature shift. While most large-budded *pcs1*^{td} cells were observed to contain no spindles at 4 and 6 h after the shift, most large-budded *cim3-1* and *cim5-1* cells contained short spindles at these time points. Incidentally, we also observed cytoplasmic microtubule arrays in the *cim3-1* cells containing short spindles that were broader and more elongated than those seen in wild-type or *cim5-1* cells; this characteristic of *cim3-1* is also apparent in the figure from the original paper describing these mutants (31). More strikingly, these data demonstrate that loss of *PCS1* function causes an arrest that differs distinctly from that caused by loss of *CIM3* or *CIM5* function.

To learn more about how loss of *PCS1* function perturbs spindle formation, we used serial section EM to examine cells from strain YHM11.2 (*pcs1*^{td}) held at 37°C for 9 h. We found that the majority of cells (21/25 examined) had failed to duplicate their SPBs and therefore possessed only a monopolar spindle. The remaining cells (4/25) had duplicated their SPBs and each contained a bipolar spindle. Fig. 9 *A* shows one pole of a bipolar spindle from one of these latter cells. The SPB seen here is indistinguishable from that of wild type: its half-bridge (*arrow*), the darkly staining segment of the nuclear envelope immediately adjacent to the SPB, has the same appearance as that which is normally seen in wild-type cells (7). Fig. 9, *B*, *B′* and *C*, *C′*, show (in adjacent sections) the single SPBs from two cells containing monopolar spindles. These SPBs are larger than normal, as has been observed for other mutants that fail to duplicate their SPBs (e.g., 8, 101). Normal half-bridge structures were not seen in any of the cells (n = 21) containing unduplicated SPBs; instead, most cells examined contained an unusual type of structure in one of the adjacent sections in the series. This structure, shown in Fig. 9, *B′* and *C′*, appears to represent an aberrant half-bridge that is unusually curved in profile and is wrapped partly around the SPB.

A GFP–Pcs1p Fusion Is Localized to the Nucleus

To gain more insight into Pcs1p function, we determined

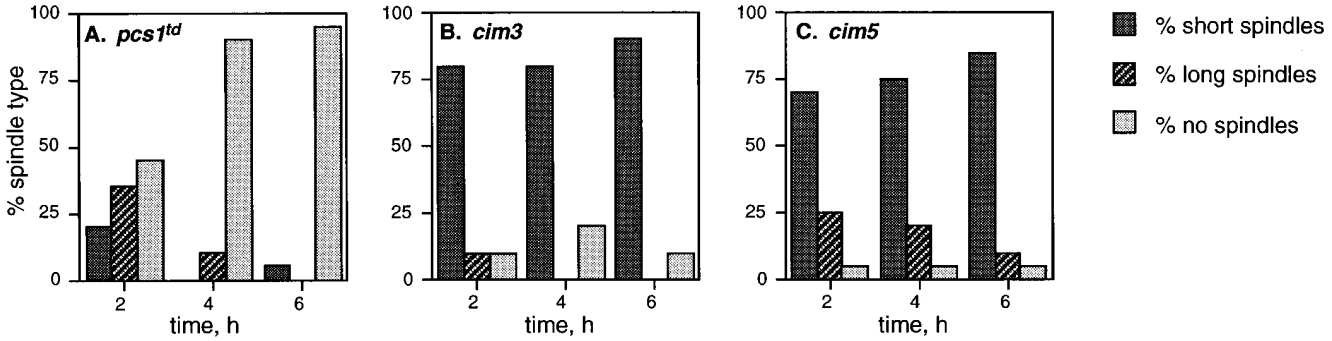

Figure 8. Spindle morphology in (*A*) YHM11.2 (*pcs1^{td}*), (*B*) CMY763 (*cim3-1*), and (*C*) CMY765 (*cim5-1*) strains at 37°C. (*Bars*) Percentages of large-budded cells with the indicated spindle forms.

the localization of a GFP–Pcs1p fusion. Plasmid pHM54 was constructed to contain the sequence encoding this fusion in a *CEN*-based vector marked with *LEU2* (see Materials and Methods). This plasmid was transformed into haploid yeast strain YHM10.1.49, which contains a disrupted chromosomal *PCS1* gene and is rendered viable by the presence of *PCS1* on a *URA3*-marked *CEN* plasmid. Leu$^+$ transformants were transferred to growth on 5-FOA, which kills cells that are Ura3$^+$ (5), effectively selecting for loss of the *URA3*-marked plasmid. The generation of 5-FOA–resistant colonies indicated that cells can use the GFP–Pcs1p fusion as their only functional source of Pcs1p. One of these isolates was retained for further analysis and designated YHM10.1.54. In this strain, GFP–Pcs1p is probably not being expressed to a significantly higher level than Pcs1p in a wild-type strain, both because its expression is controlled by the *PCS1* promoter and because it is borne on a *CEN* vector, which should be present at only one or two copies per cell (95).

The GFP–Pcs1p fusion is predicted to have a molecular mass of 76 kD. To confirm the presence of this product in strain YHM10.1.54, equivalent amounts of whole-cell extracts from strains YHM10.1.54 and Wx257-5c (wild-type control) were analyzed by Western blot (Fig. 10 *A*). Anti-GFP antiserum recognized a band of approximately the correct size in YHM10.1.54 extract (Fig. 10 *A*, lane *2*) but not in the wild-type control (lane *1*).

An asynchronous YHM10.1.54 culture was stained with DAPI to visualize DNA and examined by fluorescence microscopy. The GFP signal colocalized with the nuclear DNA, indicating that the GFP–Pcs1p fusion resides principally within the nucleus (Fig. 10, *B* and *C*). (A similar GFP signal was observed in cells that were not stained with DAPI, confirming that this signal was not due to bleed-through of the DAPI signal.) This colocalization was consistently seen in all stages of the cell cycle, including the unbudded (*1*), small-budded (*2*), and large-budded (*3* and *4*) cells indicated in the figure. The GFP signal in cell 3 is observed to colocalize with a thin finger of DNA that extends through the bud neck, as well as with the bulk of the DNA. In ~5% of the cells examined, an additional patch of GFP signal was observed at a position separate from the site of DNA staining, as indicated (*) in Fig. 10 *B*. The cytological basis for this occasional patch of apparent cytoplasmic localization is unknown, and it remains possible that it represents an extension of the nucleus. Nevertheless, it is clear that the great majority of GFP–Pcs1p fusion colocalizes with the nuclear DNA and must therefore reside within the nucleus.

To gain a better understanding of how Pcs1p distribution compares with that of other proteasome subunits, we examined the localization of a different 19S subunit. The Sen3 protein from *S. cerevisiae* is a component of the proteasome cap, unrelated in sequence to the ATPase subunits (16). To study the localization of this protein, we used MHY851 cells, which express a functional Sen3 protein tagged with three copies of the HA epitope (16). We used anti-HA antibodies to visualize Sen3 protein distribution in these cells and found that it also colocalized with the nuclear DNA throughout the cell cycle (Fig. 11, *A* and *B*). No staining was observed in cells expressing untagged Sen3 protein (strain MHY849; data not shown). Similarly, the Sug1/Cim3 and Cim5 proteins have been localized primarily to the nucleus using affinity-purified antibodies, although more significant cytoplasmic staining was observed for Cim5 than for Cim3 (Mann, C., personal communication). Thus, a number of different proteasome cap subunits appear to localize largely within the nucleus.

Discussion

We have described the identification and characterization of *PCS1*, an essential yeast gene whose predicted product shows a high level of sequence identity with a family of ATPases that are components of the 19S proteasome cap. The 67% identity between Pcs1p and p42, a known human 26S proteasome regulatory subunit (25), provides strong evidence that Pcs1p is itself a proteasome subunit. This idea has recently been confirmed biochemically (83). The p42 subunit has been identified not only as a component of the proteasome cap (also known as PA700) but also of the proteasome "modulator," a second complex that enhances cap activation of proteolytic activity (18). Whether a modulator of this sort also exists in *S. cerevisiae* is unknown.

It has been suggested that different ATPases within the 19S cap might serve to recognize distinct degradation substrates; a structural model for how this recognition specificity might be mediated has been proposed by Rech-

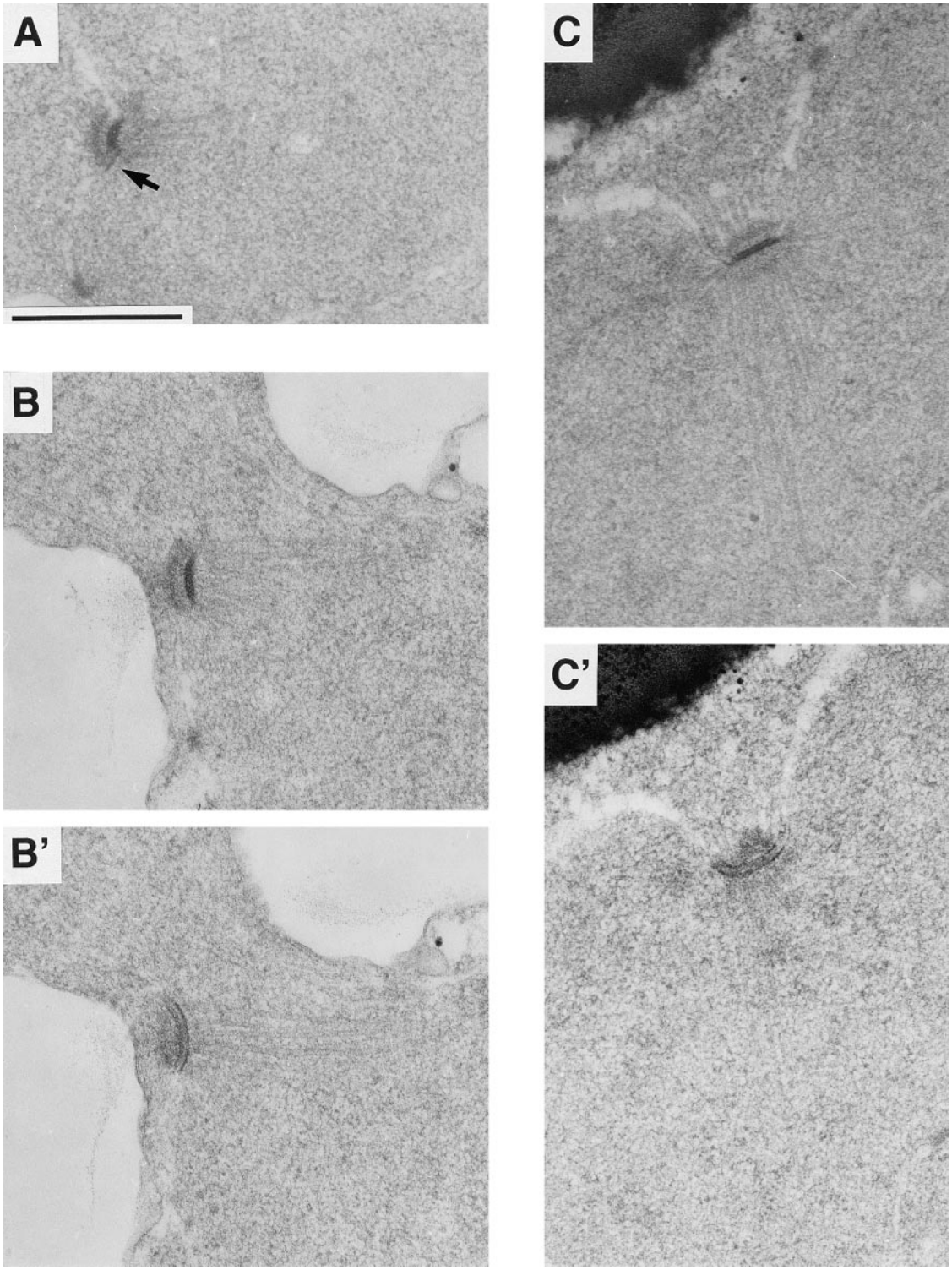

Figure 9. Electron micrographs of the YHM11.2 (*pcs1^{td}*) mutant after transfer to 37°C. A normal mitotic spindle was seen in 16% of the cells analyzed, as shown in *A*. In this cell, the other SPB was located in a different section (not shown). The arrow indicates the half-bridge structure adjacent to the SPB. Pairs of images (*B*, *B′* and *C*, *C′*) represent adjacent serial sections through the poles of monopolar spindles, as were seen in 84% of arrested cells. Bar, 0.5 μm.

steiner et al. (78). These authors note that members of this family are highly conserved in their COOH-terminal regions and more divergent in their NH_2-terminal segments (see Fig. 3), suggesting that the latter portion of the molecule might be involved in specific substrate selection. As is also the case for Pcs1p, these NH_2-terminal domains contain stretches of sequence that are predicted to form leucine zippers or α-helical coiled-coils. Rechsteiner et al. pro-

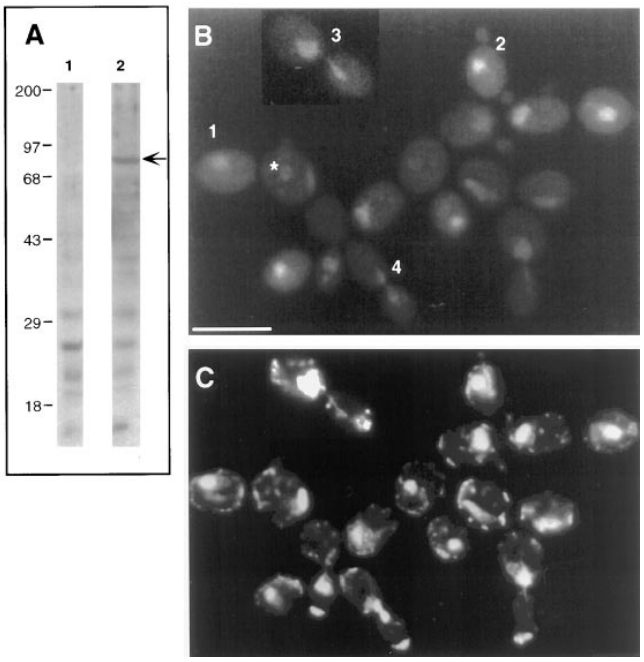

Figure 10. GFP–Pcs1p expression and localization. (*A*) Western blot analysis of whole-cell extracts probed with anti-GFP antiserum. (Lane *1*) Wx257-5c (*PCS1*). (Lane *2*) YHM10.1.54 (*GFP–PCS1*). The presumptive GFP–Pcs1p fusion is indicated by the arrow, and size markers are in kD. (*B* and *C*) Fluorescence microscopy of YHM10.1.54 cells. (*B*) GFP (FITC channel). (*1*) Unbudded cell; (*2*) small-budded cell; (*3* and *4*) large-budded cells. (*Asterisk*) Less typical (~5% of cells) appearance of GFP signal that is not coincident with nuclear DNA staining. (*C*) DNA (DAPI). Bar, 5 μm.

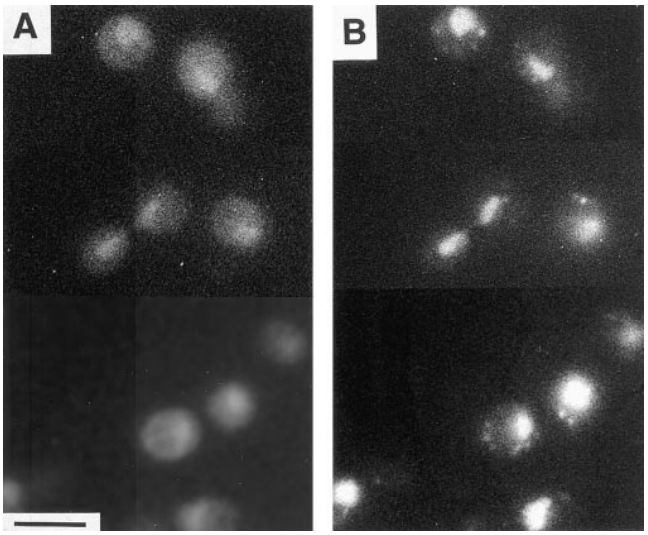

Figure 11. Sen3 protein localization. (*A*) MHY851 cells were stained with anti-HA antibody to visualize the Sen3 protein (FITC). (*B*) DNA (DAPI). Bar, 5 μm.

pose a "helix shuffle" hypothesis, in which these regions of the ATPase subunits interact with similar regions within target proteins. ATP hydrolysis would then serve to reverse this binding and to permit transfer of the substrates to the 20S proteasome core. In partial confirmation of this model, it has been shown that the leucine zipper in the murine homolog of Sug1/Cim3 protein interacts with the leucine zipper in c-Fos; both were detected in a 26S proteasome preparation (100), suggesting that murine Sug1/Cim3 may be involved in the degradation of c-Fos.

Genetic analysis supports the concept that different cap subunits might serve to recognize different substrates that have been targeted for degradation. At the restrictive temperature, *pcs1^{td}* strains are arrested in the cell division cycle as large-budded cells with replicated, unsegregated DNA that is localized to the bud neck. Surprisingly, these cells do not form bipolar spindles, although cytoplasmic microtubule staining is clearly seen. The same phenotype has been seen for a temperature-sensitive allele of *pcs1* generated by hydroxylamine mutagenesis (McDonald, H.B., and B. Byers, unpublished observations). Using EM, we determined that *pcs1^{td}* cells fail to duplicate their SPBs. This phenotype differs strikingly both from any stage seen in normal cell cycle progression and from the arrests caused by *cim3* and *cim5.* The *SUG1*/*CIM3* and *CIM5* gene products from *S. cerevisiae* are 19S cap subunits and are closely related to Pcs1p (Fig. 3). Conditional *cim3* and *cim5* mutations cause a cell to arrest in G2/M with a large bud and a short spindle (31), a state that is quite similar to that seen at the G2/M transition in a normal ongoing cell cycle. This phenotype suggests that the wild-type products of these genes play an active role in the degradation of APC-targeted substrates. Compatible with this view, the levels of B-type cyclins are increased in *cim3* and *cim5* mutants relative to wild type, even if the mutants are maintained in exponential growth at the permissive temperature (31). Since cyclin destruction is required for exit from mitosis, but not for initiation of anaphase (45, 91), the Sug1/Cim3 and Cim5 gene products are presumed to act in the degradation of other substrate(s) besides the cyclins. The distinctive *pcs1^{td}* mutant phenotype suggests, on the other hand, that Pcs1p is required for the destruction of yet another class of substrate(s).

There is precedent for mutations in different proteasomal cap subunits differing in their effects on cell cycle regulation. The *NIN1* gene of *S. cerevisiae* encodes a regulatory subunit of the 26S proteasome, but this protein is structurally unrelated to the family of ATPases that includes the *SUG1*/*CIM3* and *CIM5* products (55). Although the majority of *nin1* cells arrest at the G2/M stage of the cell cycle, the nature of this arrest is distinct from that caused by *cim3* or *cim5.* Arrested *cim3* and *cim5* mutants show activation of Cdc28p kinase, the *S. cerevisiae* CDK (31), consistent with the increased levels of mitotic cyclins observed in these mutants. In contrast, Cdc28p kinase is not activated in *nin1* mutant cells after a shift to the restrictive temperature. The basis for this difference is unknown, but an intriguing suggestion offered is that *NIN1* function is specifically required for the degradation of a CDK inhibitor (55).

The effectiveness of the *pcs1^{td}* temperature-sensitive allele supports the idea that *PCS1* function is dispensable for the degradation one particular substrate, the degron–Pcs1p fusion. Initially we were hesitant to attempt the construction of a temperature-sensitive *PCS1* allele using the

degron-based method, because degron fusions are targeted for proteolysis at high temperature by the N-end rule/ubiquitin/proteasome system. We therefore feared it might not be possible to deplete Pcs1p levels sufficiently by this technique, as Pcs1p might be required to play a role in its own destruction. However, we have identified conditions in which fully half the population of *pcs1^{td}* cells will arrest during the first division cycle after shift to high temperature, suggesting that the degron–Pcs1p fusion probably is not a component of the proteolytic machinery that is needed for its destruction.

If different cap subunits are indeed responsible for the degradation of distinct substrates, several possible models could account for this phenomenon. For example, there might exist within the cell multiple subpopulations of 26S proteasomes, each containing different cap subunits responsible for the degradation of a specific set of substrates. Distinct subpopulations of proteasomes were suggested by recent experiments in *Manduca sexta*, where levels of 19S ATPases were found to vary differentially during development (15). An alternative model would be that all 26S proteasomes in yeast are identical, with different subunits within the proteasome cap being responsible for the recognition and import of different classes of substrates. Regardless of which model proves true, the largely nuclear localization of this and certain other 19S cap subunits supports the idea that a substantial fraction of fully assembled 26S proteasomes reside within the yeast nucleus. These findings suggest, in turn, that the majority of substrates targeted for degradation may also be localized to the yeast nucleus. More specifically, we propose that Pcs1p is required for the degradation of yet to be identified nuclear substrate(s), and that this activity is required for SPB duplication to occur.

Strikingly, this work has added a new member to the small collection of yeast genes for which conditional mutations specifically perturb the process of SPB duplication while permitting other early cell cycle functions to proceed unabated. Several distinct patterns of failure in SPB duplication are seen among these mutants. In the pattern displayed by *mps2* (101) and *ndc1* (102) mutants, a nascent SPB is assembled on the half-bridge, but it fails to be inserted into the nuclear envelope. In contrast, mutations in *CDC31* (8), *KAR1* (80), and *MPS1* (101) prevent formation of the satellite, which serves as the precursor for the nascent SPB. The half-bridge in *mps1* cells is dramatically enlarged relative to the more normal-appearing half-bridge found in *cdc31-1* or *kar1* cells at temperature-sensitive arrest. *pcs1^{td}* cells likewise lack a normal half-bridge structure, but in this case the aberrant half-bridge is distinctively curvilinear in profile. Thus, mutations in these genes appear to alter the nature of half-bridge formation in different ways, each of which leads to failure of satellite formation and SPB duplication. In the case of *pcs1^{td}*, we hypothesize that some nuclear factor(s) must be degraded for half-bridge formation to proceed correctly. Further experiments would be needed to identify the relevant substrate(s) and to test other possible roles for this cap component.

We thank Drs. J. Dohmen, A. Varshavsky, M. Moser, R. Tsien, R. Heim, and F. Russo for gifts of plasmids, and Drs. M. Hochstrasser and C. Mann for yeast strains. We also thank Dr. C. Mann for communicating results prior to publication, L. Goetsch for her generous help with EM, Drs. L. Dirick and R. Coyne for useful discussions, and two anonymous reviewers for their useful comments.

This work was supported by a National Institutes of Health (NIH) postdoctoral fellowship (GM16027) to H.B. McDonald and an NIH research grant (GM18541) to B. Byers.

Received for publication 4 October 1996 and in revised form 24 February 1997.

References

1. Alber, T. 1992. Structure of the leucine zipper. *Curr. Opin. Gen. Dev.* 2: 205–210.
2. Altschul, S.F., W. Gish, W. Miller, E.W. Myers, and D.J. Lipman. 1990. Basic local alignment search tool. *J. Mol. Biol.* 215:403–410.
3. Bachmair, A., D. Finley, and A. Varshavsky. 1986. In vivo half-life of a protein is a function of its amino-terminal residue. *Science (Wash. DC).* 234:179–186.
4. Baum, P., C. Furlong, and B. Byers. 1986. Yeast gene required for spindle pole body duplication: homology of its product with Ca^{2+}-binding proteins. *Proc. Natl. Acad. Sci. USA.* 83:5512–5516.
5. Boeke, J.D., F. LaCroute, and G.R. Fink. 1984. A positive selection for mutants lacking orotidine-5′-phosphate decarboxylase activity in yeast: 5-fluoro-orotic acid resistance. *Mol. Gen. Genet.* 197:345–346.
6. Brown, K.D., R.M. Coulson, T.J. Yen, and D.W. Cleveland. 1994. Cyclin-like accumulation and loss of the putative kinetochore motor CENP-E results from coupling continuous synthesis with specific degradation at the end of mitosis. *J. Cell Biol.* 125:1303–1312.
7. Byers, B. 1981. Cytology of the yeast life cycle. *In* Molecular Biology of the Yeast *Saccharomyces.* J.N. Strathern, E.W. Jones, and J.R. Broach, editors. Cold Spring Harbor Laboratory, Cold Spring Harbor, NY. 59–96.
8. Byers, B. 1981. Multiple roles of the spindle pole bodies in the life cycle of *Saccharomyces cerevisiae. In* Molecular Genetics in Yeast, Alfred Benzon Symposia 16. D. von Wettstein, J. Friis, M. Kielland-Brandt, and A. Stenderup, editors. Munksgaard, Copenhagen. 119–133.
9. Byers, B., and L. Goetsch. 1991. Preparation of yeast cells for thin-section electron microscopy. *In* Methods in Enzymology. Vol. 194. C. Guthrie and G.R. Fink, editors. Academic Press, Inc., San Diego, CA. 602–607.
10. Chen, B., and A.E. Przybyla. 1994. An efficient site-directed mutagenesis method based on PCR. *Biotechniques.* 17:657–659.
11. Chen, P., and M. Hochstrasser. 1995. Biogenesis, structure and function of the yeast 20S proteasome. *EMBO (Eur. Mol. Biol. Organ.) J.* 14:2620–2630.
12. Chien, C.-t., P.L. Bartel, R. Sternglanz, and S. Fields. 1991. The two-hybrid system: a method to identify and clone genes for proteins that interact with a protein of interest. *Proc. Natl. Acad. Sci. USA.* 88:9578–9582.
13. Ciechanover, A. 1994. The ubiquitin-proteasome proteolytic pathway. *Cell.* 79:13–21.
14. Cohen-Fix, O., J.M. Peters, M.W. Kirschner, and D. Koshland. 1996. Anaphase initiation in *Saccharomyces cerevisiae* is controlled by the APC-dependent degradation of the anaphase inhibitor Pds1p. *Genes & Dev.* 10:3081–3093.
15. Dawson, S.P., J.E. Arnold, N.J. Mayer, S.E. Reynolds, M.A. Billett, C. Gordon, L. Colleaux, P.M. Kloetzel, K. Tanaka, and R.J. Mayer. 1995. Developmental changes of the 26 S proteasome in abdominal intersegmental muscles of *Manduca sexta* during programmed cell death. *J. Biol. Chem.* 270:1850–1858.
16. DeMarini, D.J., F.R. Papa, S. Swaminathan, D. Ursic, T.P. Rasmussen, M.R. Culbertson, and M. Hochstrasser. 1995. The yeast *SEN3* gene encodes a regulatory subunit of the 26S proteasome complex required for ubiquitin-dependent protein degradation in vivo. *Mol. Cell. Biol.* 15: 6311–6321.
17. DeMartino, G.N., and C.A. Slaughter. 1994. Regulatory proteins of the proteasome. *Enzyme Protein.* 47:314–324.
18. DeMartino, G.N., R.J. Proske, C.R. Moomaw, A.A. Strong, X. Song, H. Hisamatsu, K. Tanaka, and C.A. Slaughter. 1996. Identification, purification, and characterization of a PA700-dependent activator of the proteasome. *J. Biol. Chem.* 271:3112–3118.
19. Deveraux, Q., V. Ustrell, C. Pickart, and M. Rechsteiner. 1994. A 26S protease subunit that binds ubiquitin conjugates. *J. Biol. Chem.* 269: 7059–7061.
20. Dick, L.R., C. Aldrich, S.C. Jameson, C.R. Moomaw, B.C. Pramanik, C.K. Doyle, G.N. DeMartino, M.J. Bevan, J.M. Forman, and C.A. Slaughter. 1994. Proteolytic processing of ovalbumin and β-galactosidase by the proteasome to yield antigenic peptides. *J. Immunol.* 152: 3884–3894.
21. Dohmen, R.J., P. Wu, and A. Varshavsky. 1994. Heat-inducible degron: a method for constructing temperature-sensitive mutants. *Science (Wash. DC).* 263:1273–1276.
22. Dornitzer, D., B. Raboy, R.G. Kulka, and G.R. Fink. 1994. Regulated degradation of the transcription factor Gcn4. *EMBO (Eur. Mol. Biol. Organ.) J.* 13:6021–6030.

23. Dubiel, W., K. Ferrell, G. Pratt, and M. Rechsteiner. 1992. Subunit 4 of the 26 S protease is a member of a novel eukaryotic ATPase family. *J. Biol. Chem.* 267:22699–22702.
24. Fehling, H.J., W. Swat, C. Laplace, R. Kühn, K. Rajewsky, U. Müller, and H.V. Boehmer. 1994. MHC class I expression in mice lacking the proteasome subunit LMP-7. *Science (Wash. DC).* 265:1234–1237.
25. Fujiwara, T., T.K. Watanabe, K. Tanaka, C.A. Slaughter, and G.N. DeMartino. 1996. cDNA cloning of p42, a shared subunit of two proteasome regulatory proteins, reveals a novel member of the AAA protein family. *FEBS Lett.* 387:184–188.
26. Funabiki, H., H. Yamano, K. Kumada, K. Nagao, T. Hunt, and M. Yanagida. 1996. Cut2 proteolysis required for sister-chromatid separation in fission yeast. *Nature (Lond.).* 381:438–441.
27. Gallant, P., and E.A. Nigg. 1992. Cyclin B2 undergoes cell cycle–dependent nuclear translocation and, when expressed as a nondestructable mutant, causes mitotic arrest in HeLa cells. *J. Cell Biol.* 117:213–224.
28. Ganoth, D., E. Leshinsky, E. Eytan, and A. Hershko. 1988. A multicomponent system that degrades proteins conjugated to ubiquitin. Resolution of factors and evidence for ATP-dependent complex formation. *J. Biol. Chem.* 263:12412–12419.
29. Garnier, J., D.J. Osguthorpe, and B. Robson. 1978. Analysis of the accuracy and implications of simple methods for predicting the secondary structure of globular proteins. *J. Mol. Biol.* 120:97–120.
30. Ghiara, J.B., H.E. Richardson, K. Sugimoto, M. Henze, D.J. Lew, C. Wittenberg, and S.I. Reed. 1991. A cyclin B homolog in *S. cerevisiae*: chronic activation of the Cdc28 protein kinase by cyclin prevents exit from mitosis. *Cell.* 65:163–174.
31. Ghislain, M., A. Udvardy, and C. Mann. 1993. *S. cerevisiae* 26S protease mutants arrest cell division in G2/metaphase. *Nature (Lond.).* 366:358–362.
32. Glotzer, M., A.W. Murray, and M.W. Kirschner. 1991. Cyclin is degraded by the ubiquitin pathway. *Nature (Lond.).* 349:132–138.
33. Goldberg, A.L. 1995. Functions of the proteasome: the lysis at the end of the tunnel. *Science (Wash. DC).* 268:522–523.
34. Gonda, D.K. 1994. Molecular genetics of the ubiquitin system. *In* Cellular Proteolytic Systems. Vol. 15. A.J. Ciechanover and A.L. Schwartz, editors. Wiley-Liss, Inc. 23–51.
35. Gordon, C., G. McGurk, P. Dillon, C. Rosen, and N.D. Hastle. 1993. Defective mitosis due to a mutation in the gene for a fission yeast 26S protease subunit. *Nature (Lond.).* 366:355–357.
36. Genetics Computer Group. 1994. Program Manual for the Wisconsin Package. Madison, WI.
37. Hartwell, L.H. 1967. Macromolecule synthesis in temperature-sensitive mutants of yeast. *J. Bacteriol.* 93:1662–1670.
38. Heim, R., A.B. Cubitt, and R.Y. Tsien. 1995. Improved green fluorescence [letter]. *Nature (Lond.).* 373:663–664.
39. Hershko, A., D. Ganoth, V. Sudakin, A. Dahan, L.H. Cohen, F.C. Luca, J.V. Ruderman, and E. Eytan. 1994. Components of a system that ligates cyclin to ubiquitin and their regulation by the protein kinase cdc2. *J. Biol. Chem.* 269:4940–4946.
40. Hicke, L., and H. Riezman. 1996. Ubiquitination of a yeast plasma membrane receptor signals its ligand-stimulated endocytosis. *Cell.* 84:277–287.
41. Hilt, W., W. Heinemeyer, and D.H. Wolf. 1994. Studies on the yeast proteasome uncover its basic structural features and multiple in vivo functions. *Enzyme Protein.* 47:189–201.
42. Hochstrasser, M. 1995. Ubiquitin, proteasomes, and the regulation of intracellular protein degradation. *Curr. Opin. Cell Biol.* 7:215–223.
43. Hochstrasser, M., and A. Varshavsky. 1990. In vivo degradation of a transcriptional regulator: the yeast α2 repressor. *Cell.* 61:697–708.
44. Hochstrasser, M., M.J. Ellison, V. Chau, and A. Varshavsky. 1991. The short-lived MATα2 transcriptional regulator is ubiquitinated in vivo. *Proc. Natl. Acad. Sci. USA.* 88:4606–4610.
45. Holloway, S.L., M. Glotzer, R.W. King, and A.W. Murray. 1993. Anaphase is initiated by proteolysis rather than by the inactivation of maturation-promoting factor. *Cell.* 73:1393–1402.
46. Huang, Y., R.T. Baker, and J.A. Fischer-Vize. 1995. Control of cell fate by a deubiquitinating enzyme encoded by the *fat facets* gene. *Science (Wash. DC).* 270:1828–1830.
47. Hutter, K.J., and H.E. Eipel. 1979. Microbial determination by flow cytometry. *J. Gen. Microbiol.* 113:369–375.
48. Irniger, S., S. Piatti, C. Michaelis, and K. Nasmyth. 1995. Genes involved in sister chromatid separation are needed for B-type cyclin proteolysis in budding yeast. *Cell.* 81:269–277.
49. Jacobs, C.W., A.E.M. Adams, P.J. Szaniszlo, and J.R. Pringle. 1988. Functions of microtubules in the *Saccharomyces cerevisiae* cell cycle. *J. Cell Biol.* 107:1409–1426.
50. Jentsch, S., and S. Schlenker. 1995. Selective protein degradation: a journey's end within the proteasome. *Cell.* 82:881–884.
51. Kilmartin, J.V., and A.E.M. Adams. 1984. Structural rearrangements of tubulin and actin during the cell cycle of the yeast *Saccharomyces. J. Cell Biol.* 98:922–933.
52. King, R.W., J.-M. Peters, S. Tugendreich, M. Rolfe, P. Hieter, and M.W. Kirschner. 1995. A 20S complex containing CDC27 and CDC16 catalyzes the mitosis-specific conjugation of ubiquitin to cyclin B. *Cell.* 81: 279–288.
53. King, R.W., R.J. Deshaies, J.-M. Peters, and M.W. Kirschner. 1996. How proteolysis drives the cell cycle. *Science (Wash. DC).* 274:1652–1658.
54. Kolling, R., and C.P. Hollenberg. 1994. The ABC-transporter Ste6 accumulates in the plasma membrane in a ubiquitinated form in endocytosis mutants. *EMBO (Eur. Mol. Biol. Organ.) J.* 13:3261–3271.
55. Kominami, K., G.N. DeMartino, C.R. Moomaw, C.A. Slaughter, N. Shimbara, M. Fujimuro, H. Yokosawa, H. Hisamatsu, N. Tanahashi, Y. Shimizu et al. 1995. Nin1p, a regulatory subunit of the 26S proteasome, is necessary for activation of Cdc28p kinase of *Saccharomyces cerevisiae. EMBO (Eur. Mol. Biol. Organ.) J.* 14:3105–3115.
56. Kunau, W.H., A. Beyer, T. Franken, K. Gotte, M. Marzioch, J. Saidowsky, A. Skaletz-Rorowski, and F.F. Wiebel. 1993. Two complementary approaches to study peroxisome biogenesis in *Saccharomyces cerevisiae*: forward and reversed genetics. *Biochimie (Paris).* 75:209–224.
57. Kyte, J., and R.F. Doolittle. 1982. A simple method for displaying the hydropathic character of a protein. *J. Mol. Biol.* 157:105–132.
58. Laemmli, U.K. 1970. Cleavage of structural proteins during the assembly of the head of bacteriophage T4. *Nature (Lond.).* 227:680–685.
59. Lamb, J.R., W.A. Michaud, R.S. Sikorski, and P.A. Hieter. 1994. Cdc16p, Cdc23p and Cdc27p form a complex essential for mitosis. *EMBO (Eur. Mol. Biol. Organ.) J.* 13:4321–4328.
60. Löwe, J., D. Stock, B. Jap, P. Zwickl, W. Baumeister, and R. Huber. 1995. Crystal structure of the 20S proteasome from the archaeon *T. acidophilum* at 3.4 Å resolution. *Science (Wash. DC).* 268:533–539.
61. Luca, F.C., E.K. Shibuya, C.E. Dohrmann, and J.V. Ruderman. 1991. Both cyclin AΔ60 and BΔ97 are stable and arrest cells in M-phase, but only cyclin BΔ97 turns on cyclin destruction. *EMBO (Eur. Mol. Biol. Organ.) J.* 10:4311–4320.
62. Lupas, A., M.V. Dyke, and J. Stock. 1991. Predicting coiled coils from protein sequences. *Science (Wash. DC).* 252:1162–1164.
63. Ma, C.-P., J.H. Vu, R.J. Proske, C.A. Slaughter, and G.N. DeMartino. 1994. Identification, purification, and characterization of a high molecular weight, ATP-dependent activator (PA700) of the 20S proteasome. *J. Biol. Chem.* 269:3539–3547.
64. Madura, K., and A. Varshavsky. 1994. Degradation of Gα by the N-end rule pathway. *Science (Wash. DC).* 265:1454–1458.
65. McCusker, J.H., and J.E. Haber. 1988. Cycloheximide-resistant temperature-sensitive lethal mutations of *Saccharomyces cerevisiae. Genetics.* 119:303–315.
66. Mortimer, R., and D. Hawthorne. 1969. Yeast genetics. *In* The Yeasts. Vol. 1. A.H. Rose and J.S. Harrison, editors. Academic Press, New York. 385–460.
67. Murray, A. 1995. Cyclin ubiquitination: the destructive end of mitosis. *Cell.* 81:149–152.
68. Murray, A.W., M. Solomon, and M.W. Kirschner. 1989. The role of cyclin synthesis and degradation in the control of maturation promoting factor activity. *Nature (Lond.).* 339:280–286.
69. Nakai, K., and M. Kanehisa. 1992. A knowledge base for predicting protein localization sites in eukaryotic cells. *Genomics.* 14:897–911.
70. Nigg, E.A. 1995. Cyclin-dependent protein kinases: key regulators of the eukaryotic cell cycle. *Bioessays.* 17:471–480.
71. Oh, C.E., R. McMahon, S. Benzer, and M.A. Tanouye. 1994. *bendless*, a *Drosophila* gene affecting neuronal connectivity, encodes a ubiquitin-conjugating enzyme homolog. *J. Neurosci.* 14:3166–3179.
72. Palmer, R.E., M. Koval, and D. Koshland. 1989. The dynamics of chromosome movement in the budding yeast *Saccharomyces cerevisiae. J. Cell Biol.* 109:3355–3366.
73. Palombella, V.J., O.J. Rando, A.L. Goldberg, and T. Maniatis. 1994. The ubiquitin-proteasome pathway is required for processing the NF-κB1 precursor protein and the activation of NF-κB. *Cell.* 78:773–785.
74. Pellman, D., M. Bagget, H. Tu, and G.R. Fink. 1995. Two microtubule-associated proteins required for anaphase spindle movement in *Saccharomyces cerevisiae. J. Cell Biol.* 130:1373–1385.
75. Peters, J.-M. 1994. Proteasomes: protein degradation machines of the cell. *TIBS.* 19:377–382.
76. Peters, J.-M., W.W. Franke, and J.A. Kleinschmidt. 1994. Distinct 19 S and 20 S subcomplexes of the 26 S proteasome and their distribution in the nucleus and cytoplasm. *J. Biol. Chem.* 269:7709–7718.
77. Peters, J.-M., R.W. King, C. Höög, and M.W. Kirschner. 1996. Identification of BIME as a subunit of the anaphase-promoting complex. *Science (Wash. DC).* 274:1199–1201.
78. Rechsteiner, M., L. Hoffman, and W. Dubiel. 1993. The multicatalytic and 26 S proteases. *J. Biol. Chem.* 268:6065–6068.
79. Rock, K.L., C. Gramm, L. Rothstein, K. Clark, R. Stein, L. Dick, D. Hwang, and A. Goldberg. 1994. Inhibitors of the proteasome block the degradation of most cell proteins and the generation of peptides presented on MHC class I molecules. *Cell.* 78:761–771.
80. Rose, M.D., and G.R. Fink. 1987. *KAR1*, a gene required for function of both intranuclear and extranuclear microtubules in yeast. *Cell.* 48:1047–1060.
81. Rothstein, R. 1991. Targeting, disruption, replacement, and allele rescue: integrative DNA transformation in yeast. *In* Guide to Yeast Genetics and Molecular Biology. Vol. 194. C. Guthrie and G.R. Fink, editors. Academic Press, Inc., San Diego. 281–301.
82. Rubin, D.M., O. Coux, I. Wefes, C. Hengartner, R.A. Young, A.L. Goldberg, and D. Finley. 1996. Identification of the gal4 suppressor Sug1 as a

subunit of the yeast 26S proteasome. *Nature (Lond.).* 379:655–657.
83. Russell, S.J., U.G. Sathyanarayana, and S.A. Johnston. 1996. Isolation and characterization of SUG2. *J. Biol. Chem.* 271:32810–32817.
84. Sambrook, J., E.F. Fritsch, and T. Maniatis. 1989. Molecular Cloning: A Laboratory Manual. Cold Spring Harbor Laboratory, Cold Spring Harbor, NY. 545 pp.
85. Scherer, S., and R.W. Davis. 1979. Replacement of chromosome segments with altered DNA sequences constructed in vitro. *Proc. Natl. Acad. Sci. USA.* 76:4951–4955.
86. Schnall, R., G. Mannhaupt, R. Stucka, R. Tauer, S. Ehnle, C. Schwarzlose, I. Vetter, and H. Feldmann. 1994. Identification of a set of yeast genes coding for a novel family of putative ATPases with high similarity to constituents of the 26S protease complex. *Yeast.* 10:1141–1155.
87. Shanklin, J., M. Jabben, and R.D. Vierstra. 1987. Red light-induced formation of ubiquitin-phytochrome conjugates: identification of a possible intermediate of phytochrome degradation. *Proc. Natl. Acad. Sci. USA.* 84:359–363.
88. Sikorski, R.S., and P. Hieter. 1989. A system of shuttle vectors and yeast host strains designed for efficient manipulation of DNA in *Saccharomyces cerevisiae. Genetics.* 122:19–27.
89. Stratmann, R., and C.F. Lehner. 1996. Separation of sister chromatids in mitosis requires the *Drosophila pimples* product, a protein degraded after the metaphase/anaphase transition. *Cell.* 84:25–35.
90. Sudakin, V., D. Ganoth, A. Dahan, H. Heller, J. Hershko, F.C. Luca, J.V. Ruderman, and A. Hershko. 1995. The cyclosome, a large complex containing cyclin-selective ubiquitin ligase activity, targets cyclins for destruction at the end of mitosis. *Mol. Biol. Cell.* 6:185–198.
91. Surana, U., A. Amon, C. Dowzer, J. McGrew, B. Byers, and K. Nasmyth. 1993. Destruction of the CDC28/CLB mitotic kinase is not required for the metaphase to anaphase transition in budding yeast. *EMBO (Eur. Mol. Biol. Organ.) J.* 12:1969–1978.
92. Swaffield, J.C., J.F. Bromberg, and S.A. Johnston. 1992. Alterations in a yeast protein resembling HIV Tat-binding protein relieve requirement for an acidic activation domain in GAL4. *Nature (Lond.).* 357:698–700.
93. Thomas, J.H., and D. Botstein. 1986. A gene required for the separation of chromosomes on the spindle apparatus in yeast. *Cell.* 44:65–76.
94. Treier, M., L.M. Staszewski, and D. Bohmann. 1994. Ubiquitin-dependent c-jun degradation in vivo is mediated by the δ domain. *Cell.* 78:787–798.
95. Tschumper, G., and J. Carbon. 1983. Copy number control by a yeast centromere. *Gene (Amst.).* 23:221–232.
96. Tugendreich, S., J. Tomkiel, W. Earnshaw, and P. Hieter. 1995. CDC27Hs colocalizes with CDC16Hs to the centrosome and mitotic spindle and is essential for the metaphase to anaphase transition. *Cell.* 81:261–268.
97. Vallen, E.A., T.Y. Scherson, T. Roberts, K. van Zee, and M.D. Rose. 1992. Asymmetric mitotic segregation of the yeast spindle pole body. *Cell.* 69:505–515.
98. Vojtek, A.B., S.M. Hollenberg, and J.A. Cooper. 1993. Mammalian ras interacts directly with the serine/threonine kinase raf. *Cell.* 74:205–214.
99. Walker, J.E., M. Saraste, M.J. Runswick, and N.J. Gay. 1982. Distantly related sequences in the α- and β-subunits of ATP synthase, myosin, kinases and other ATP-requiring enzymes and a common nucleotide binding fold. *EMBO (Eur. Mol. Biol. Organ.) J.* 1:945–951.
100. Wang, W., P.M. Chevray, and D. Nathans. 1996. Mammalian Sug1 and c-Fos in the nuclear 26S proteasome. *Proc. Natl. Acad. Sci. USA.* 93: 8236–8240.
101. Winey, M., L. Goetsch, P. Baum, and B. Byers. 1991. *MPS1* and *MPS2*: novel yeast genes defining distinct steps of spindle pole body duplication. *J. Cell. Biol.* 114:745–754.
102. Winey, M., M.A. Hoyt, C. Chan, L. Goetsch, D. Botstein, and B. Byers. 1993. *NDC1*: a nuclear periphery component required for yeast spindle pole body duplication. *J. Cell Biol.* 122:743–751.
103. Yamamoto, A., V. Guacci, and D. Koshland. 1996. Pds1p is required for faithful execution of anaphase in the yeast, *Saccharomyces cerevisiae. J. Cell Biol.* 133:85–97.
104. Yamamoto, A., V. Guacci, and D. Koshland. 1996. Pds1p, an inhibitor of anaphase in budding yeast, plays a critical role in the APC and checkpoint pathway(s). *J. Cell Biol.* 133:99–110.
105. Zachariae, W., T.H. Shin, M. Galova, B. Obermaier, and K. Nasmyth. 1996. Identification of subunits of the anaphase-promoting complex of *Saccharomyces cerevisiae. Science (Wash. DC).* 274:1201–1204.